Proceedings of the 17th World Congress
The International Federation of Automatic Control
Seoul, Korea, July 6-11, 2008

Temperature Control of a Tube Furnace: An Experimental Approach

Carlos A. Joers-Delgado * **Aaron Gonzalez-Rodriguez** **
Reyna Medellin-Marsuez *** **Ruben Salas-Cabrera** **

* *Instituto Tecnologico de Cd. Madero, Division de Estudios de Posgrado e Investigacion, Av. 1o. de Mayo S/N Cd. Madero, Mexico*
** *Instituto Tecnologico de Cd. Madero, Departamento de Ingenieria Electronica and Division de Estudios de Posgrado e Investigacion, Av. 1o. de Mayo S/N Cd. Madero, Mexico*
*** *Instituto Tecnologico de Cd. Madero, Departamento de Ingenieria Quimica y Bioquimica, Av. 1o. de Mayo S/N Cd. Madero, Mexico*

Abstract: This work deals with the experimental temperature control of a tube furnace that is used for determining physical and chemical properties of different compounds. Several experimental tests are performed to identify the dynamic model, then pole placement technique and integral control by state augmentation are employed to design the control law. In other words discrete time control theory is utilized to implement this temperature microprocessor-based controller. Analog, digital and power electronics are the fundamental components of the custom-made instrumentation.

1. INTRODUCTION

In industrial settings and research laboratories is common to employ a furnace as an experimental tool for determining different physical and chemical properties of compounds. Temperature is one of those critical factors that defines the conditions for the analysis of the compounds. That is why it is important to control the temperature in a reliable manner.

There are some contributions regarding the temperature control of different kind of furnaces, for example Barry et al. [1995], Grassi et al [2000], Moon et al [2003], Huaiquan et al [2006] and Gao et al [2006]. The ideas and results presented in those papers denote the creativity, engineering and the rigorous mathematical background necessary to address some of issues involved in the temperature control of furnaces.

In Moon et al [2003], authors present theoretical and experimental results when controlling a furnace that is used to manufacture glass for TV picture tubes. The dynamics of that type of furnace is clearly complex and obtaining a reliable model for designing a control law is not an easy task. A conventional PI controller is implemented in Moon et al [2003] for the linear part of the system and a fuzzy controller for the complex nonlinear dynamics. A PID tuning technique is employed in Grassi et al [2000] for controlling the temperature of a diffusion furnace used in semiconductor manufacturing. The tuning procedure is presented as a convex optimization problem in the frequency domain. The constructive characteristics of the furnace that is used in this paper are different to those described in Moon et al [2003], Grassi et al [2000] and Gao et al [2006]. In other words, the models employed in the control design are different to the one presented here. In Moon et al [2003] and Grassi et al [2000] the complexity of the control design is addressed without describing the details of the experimental implementation. In this work, we deal with an experimental development involving a controller, actuator and a measurement device for controlling a heating plant. In Gao et al [2006] a very interesting idea of a hybrid controller is presented. The genetic algorithm is used to define the initial conditions of a standard PID controller. Simulation results presented in Gao et al [2006] showed the potential future of this technique. In contrast, Huaiquan et al [2006] presented the practical implementation of a furnace control employing a dedicated real-time hardware/software. In Huaiquan et al [2006] the emphasis is on the implementation rather than on the control design. In Barry et al. [1995], an electronics scheme is described to control the temperature of an oven. In particular, an integer-cycle binary rate modulation is presented to define the AC cycles to be applied to the heating element. In terms of the experimental implementation, we use an electronics technique based on burst firing of an integer number of AC half-cycles. As established in Barry et al. [1995], this electronics-based scheme is similar to the Pulse Width Modulation PWM with discrete steps within the PWM cycle. This scheme is clearly easier to implement than that of using a standard AC-to-AC PWM converter for modifying the RMS value, Rashid [2004]. Since the well known power electronics phase control scheme is not used, no partial half-cycles are applied, therefore harmonics injection is significantly reduced, Rashid [2004]. Transfer functions are utilized in Barry et al. [1995], Grassi et al [2000] and Moon et al [2003]. In contrast, we employ a state space design involving the pole placement technique and the integral control by state augmentation.

⋆ This work was supported in part by the Instituto Tecnologico de Cd. Madero and the Fondo Mixto de Fomento a la Investigacion Cientifica y Tecnologica CONACyT-Gobierno del Estado de Tamaulipas

A brief description of this paper follows. The state space representation of the system and its corresponding input are described in Section 2. It is also established the connection between the input defined by the control law and the input that is applied to the actual furnace. Section 3 deals with the design of the control law. The main contribution of this paper is presented in Section 4 where the experimental setup is described. Experimental results of the closed loop system are shown in Section 5.

2. MODELING

The furnace we use here has a heating element embedded in a refractory material, Barnstead [1997]. The process tube, containing the compound to be investigated, is placed inside the chamber, which is insulated with a ceramic fiber insulation. The basic element used to measure the temperature in the chamber is a thermocouple, which provides a voltage that represents the temperature.

Before proceeding with the identification of this dynamic system it is appropriate to define the input in terms of a practical perspective, Barry et al. [1995].

2.1 Input

The nominal characteristics of the power supply for this tube furnace are 127 volts 60 Hz single phase. On the other hand, in order to implement a closed loop control using a discrete-time state space representation, a sampling period had to be determined. Considering the hardware and software involved in this project, it was estimated that a 3 sec sampling period was feasible. The sampling frequency, defined by $w_s = 2\pi/T$ where T is the sampling period, is then $w_s = 2.0944$ rad/sec. With the purpose of avoiding the typical roughness that appears in discrete systems, sampling frequency should be selected several times the natural frequency of the closed loop system, Franklin et al [1998]. As a design specification, the fastest rise time of the closed loop system was defined. In this particular case, it was about 450 seconds. Assuming that $w_n = 1.8/t_r$, Franklin et al [1998], where t_r is the rise time and w_n is the natural frequency, then $w_n = 0.004$ rad/sec. It is clear that the ratio $w_s/w_n \approx 523$ establishes the conditions for a succesful implementation of the control law, Ogata [1995], Franklin et al [1998]. There are 360 half-cycles occurring during the 3 sec sampling period when this 60 Hz supply is employed. In this work, the control law does not define the input of the system by modifying the RMS value (or the frequency) of the power supply. Instead, the control law defines the input by controlling the portion of the half-cycles of AC voltage to be applied within the 3 sec sampling period. The input can be positioned anywhere within the 0-1 range which corresponds to 0-360 half-cycles, respectively. In other words, a 0.0166 input means that 0.0166(360)=6 half-cycles are applied at its nominal instantaneous value and the next 354 half-cycles are removed. For illustration purposes only, this input is shown in Fig.1 for two sampling periods.

As stated before this practical input has been described as burst firing of an integer number of AC half-cycles, Barry et al. [1995]. At the same time it is important to note that the open-loop input of this system is a

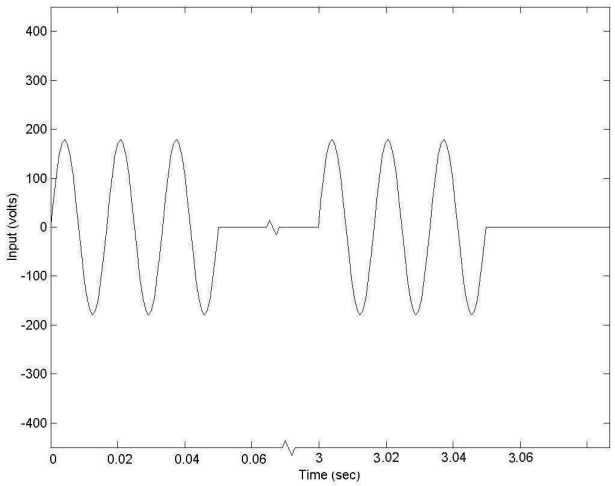

Fig. 1. 0.0166 Input with a 3 sec. sampling period

periodic sine function that depends on the time. In this work we have employed a practical input that allows us to use a standard state space representation. There is an implicit transformation that maps the input defined by the control law (and having a constant value during steady state conditions) into the input that is applied to the experimental system (and having, during a period of time at steady state conditions, a periodic sine function depending on the time).

2.2 State Space Representation

For the purpose of identifying the model of the system several step inputs were applied. Let us consider the experimental dynamic response for five different step inputs: 0.3, 0.35, 0.4, 0.45 and 0.5. These inputs correspond to 0.3*360=108, 0.35*360=126, 0.4*360=144, 0.45*360=162 and 0.5*360=180 nonzero half-cycles applied within every 3 sec sampling period. Each input was held constant for about 6000 sec. Measured transient traces are depicted in Fig. 2. It is evident that the system can be approximated by a first-order time invariant linear differential equation. Although tests were performed on the same experimental furnace, a straightforward analysis of the responses shows that different time constants are involved. Table I reflects that by showing the different parameters. Standard notation for linear state equations is used in Table I, this is $\dot{x}(t) = Ax(t) + Bu(t)$.

In order to obtain a model useful for experimental work, we decided to employ what we called a nominal model, Chen [1999]. It was calculated by averaging the different values for A and B in Table I. Then, the continuous nominal dynamic equation of the system now becomes

$$\begin{aligned} \dot{x}(t) &= -0.0011x(t) + 1.3508u(t) \\ y(t) &= x(t) \end{aligned} \tag{1}$$

where the state variable x is the temperature, the input u is the portion of half-cycles to be applied within the sampling period and the output to be controlled y is the temperature. Experimental results in Section 5 will show that the nominal model in (1) contains the fundamental dynamic characteristics of the system necessary to design

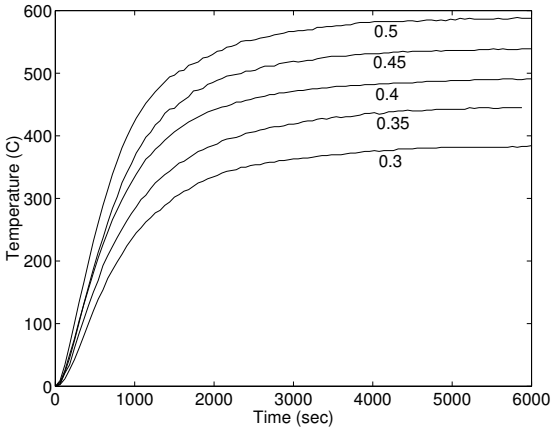

Fig. 2. Experimental response for five different step inputs

Table 1. Parameters of the State Equation

u(t)	A	B
.3	-0.001	1.2647
0.35	-0.001	1.2843
0.4	-0.0011	1.3639
0.45	-0.0011	1.3309
0.5	-0.0013	1.5103

a successful experimental control law. Parametric uncertainty, as those presented in Table 1, will be addressed by using an integrator. Now, utilizing the theory presented in Ogata [1995], Franklin et al [1998] or using the computer tools available in Mathworks [2001] the discrete representation of (1) can be calculated, i.e.

$$\begin{aligned} x(k+1) &= 0.9967x(k) + 4.0457u(k) \\ y(k) &= x(k) \end{aligned} \tag{2}$$

where a 3 sec. sampling period was used.

3. CONTROL LAW

In this section, the pole placement technique is employed for calculating the gains associated with the state vector. Also it is necessary to include a discrete integrator in order to eliminate any steady state error due to parametric related disturbances, this is

$$x_I(k+1) = x_I(k) + e(k) = x_I(k) + y(k) - r(k) \tag{3}$$

where r is the reference signal for the output y of the system. Using (2) and (3), the following discrete-time state equation of the augmented plant results

$$\begin{aligned} \begin{bmatrix} x_I(k+1) \\ x(k+1) \end{bmatrix} = \begin{bmatrix} 1 & 1 \\ 0 & 0.9967 \end{bmatrix} \begin{bmatrix} x_I(k) \\ x(k) \end{bmatrix} + \\ + \begin{bmatrix} 0 \\ 4.0457 \end{bmatrix} u(k) - \begin{bmatrix} 1 \\ 0 \end{bmatrix} r(k) \end{aligned} \tag{4}$$

where x is the state variable of the original system and x_I is the integral state variable. The discrete-time state equation (4) is said to be controllable since the controllability matrix has rank two, Ogata [1995], Franklin et al [1998], Chen [1999]. Then the closed-loop eigenvalues can be arbitrarily placed by using the following standard state feedback Ogata [1995], Franklin et al [1998], Chen [1999]

$$u(k) = -[K_I \;\; K] \begin{bmatrix} x_I(k) \\ x(k) \end{bmatrix} \tag{5}$$

Simulated dynamic behavior shown in Fig. 3 and Fig. 4 illustrate the transient response of the state variables defined by the discrete representation in (4) when the state feedback in (5) is applied. The initial conditions are $[x_I(0), x(0)] = [0, 33]$ and the reference is set equal to 172 C. In this particular case, gains in (5) were chosen such that the desired closed-loop poles become $z_{1,2} = 0.97, 0.965$, this is $[K_I, K] = [0.0003, 0.0153]$. Fig. 5 shows the simulated transient of $u(k)$ for the mentioned conditions. It is important to point out that no saturation of the input occurs during this particular transient. It is clear that the overdamped response of the state variables corresponds to the location of the desired closed-loop poles Ogata [1995] Franklin et al [1998]. A comment regarding the selection of the closed loop poles will be established in Section 5. Next section we will present the main contribution of this work, i.e. the practical implementation of this control law.

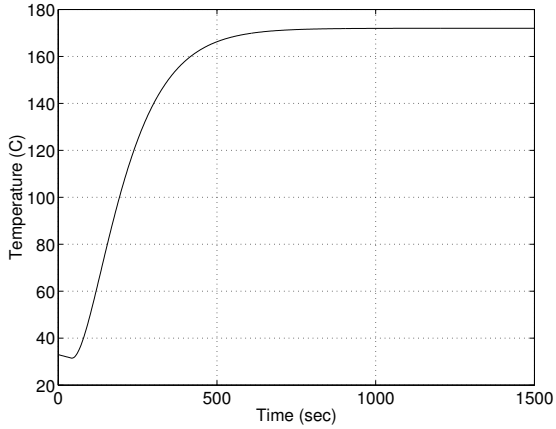

Fig. 3. Simulated response of temperature versus time. Closed loop poles: $z_{1,2} = 0.97, 0.965$.

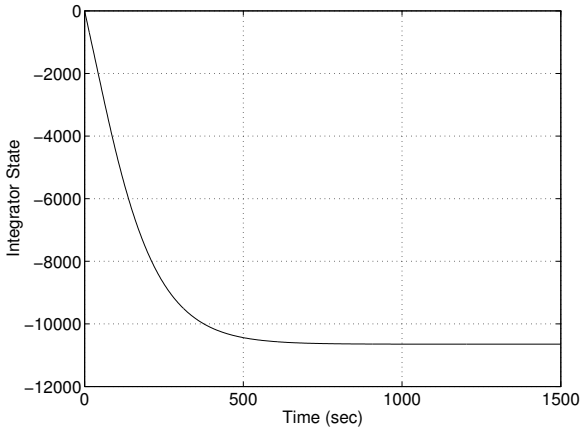

Fig. 4. Simulated response of integral error versus time

4. EXPERIMENTAL SETUP

In this part of the paper we describe the custom-made instrumentation necessary for implementing this closed loop system. As established earlier a variety of analog, digital and power electronics Integrated Circuits (IC's) and components were interconnected to perform different tasks in this design, Rashid [2004], Coughlin et al [2001], Boylestad

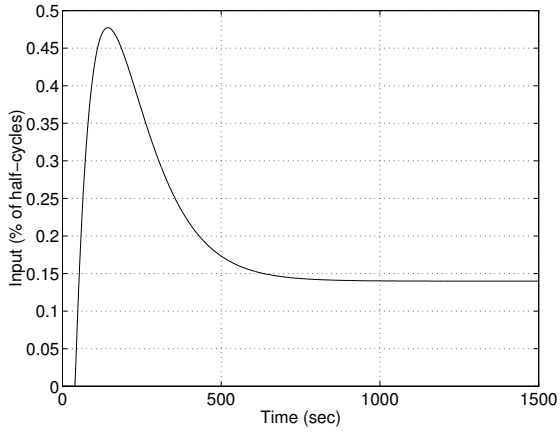

Fig. 5. Simulated response of input versus time

et al [2006]. A list of the most important IC's/components follows: Microcontroller AT89S8252, Zero crossing optoisolator triac driver MOC3031, Precision centigrade temperature sensor LM35, Precision operational amplifier OP-07, A/D Converter with input multiplexer and sample/hold ADC10062, Liquid crystal display LCD Lumex LCM S01602DTR, 40 Amp. power Triac NTE56026, Jfet-input operational amplifier TL081 and a type K chromel/alumel thermocouple. A brief description of the electronic design represented by the block diagram in Fig. 6, follows:

-Microprocessor. This is the central processing unit that

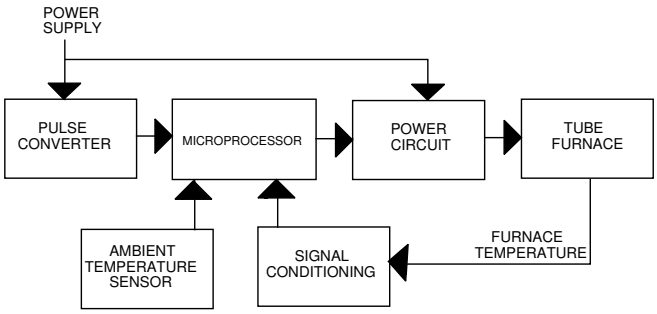

Fig. 6. Block diagram of the experimental setup

calculates the input of the system for every sampled period. Basically, it solves the state feedback in (5) based on the integral state variable and the measured temperature. In order to have the controller state variable, it is clear that difference equation in (3) has to be computed. Reference signal r is specified using the keyboard and is obtained by the microprocessor through a digital port. All the calculations that are performed by the microprocessor were done employing assembler language and the hexadecimal number system. The following figure depicts the schematics of the microprocessor and some of the connections to and from the other electronic components.

-Pulse converter circuit. As noted in Fig. 8, the input signal of this circuit is a low level AC voltage proportional to the voltage at the power supply. The output signal has a pulse every time the power voltage passes through zero. This output is connected to the microprocessor, which uses the signal for implementing the control law that defines the number of half-cycles to be applied.

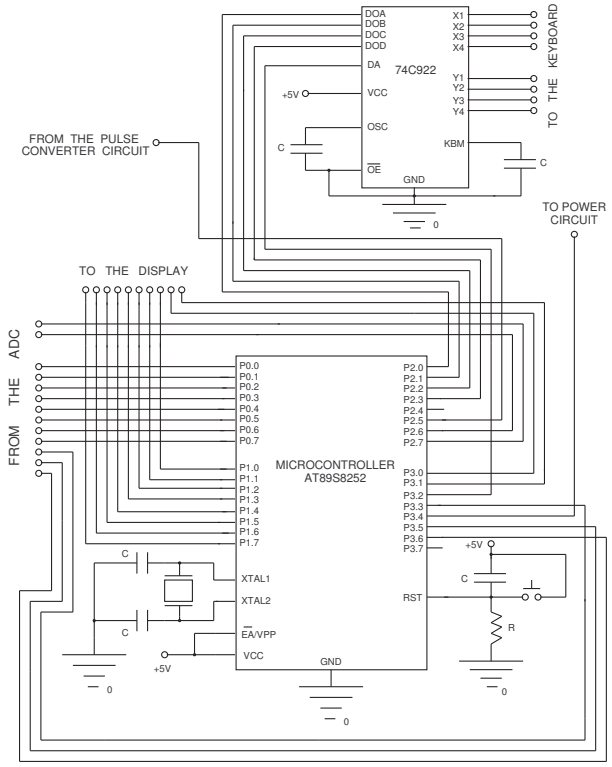

Fig. 7. Wiring diagram of the microprocessor

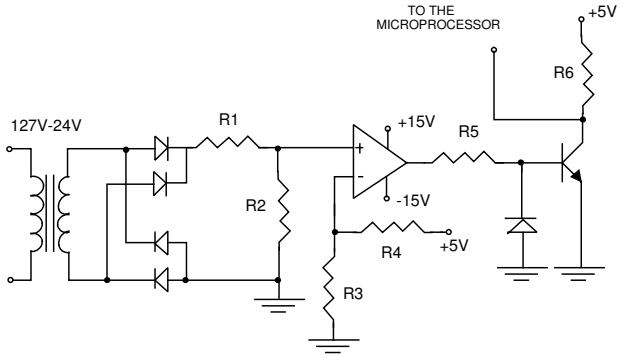

Fig. 8. Pulse converter circuit

-Signal Conditioning. Some of the purposes of this section of the electronic design is to amplify and filter the voltage measured at the thermocouple terminals. In this part of the circuit, that analog signal is also converted to its digital format in order to be interpreted by the microprocessor. This measurement of the original non-augmented state variable is clearly necessary for calculating the integral state variable in (3) and the state feedback in (5). A part of the signal conditioning circuit is illustrated in Fig. 9.

-Power circuit. Basically, this section consists of an isolator that optically turns on the power triac. The period of time that the power element is switched on is defined by the control law implemented in the microprocessor.

-Display and keyboard. These devices are included in this

design for setting up the controller and monitoring the steady state and transient behavior of the temperature.

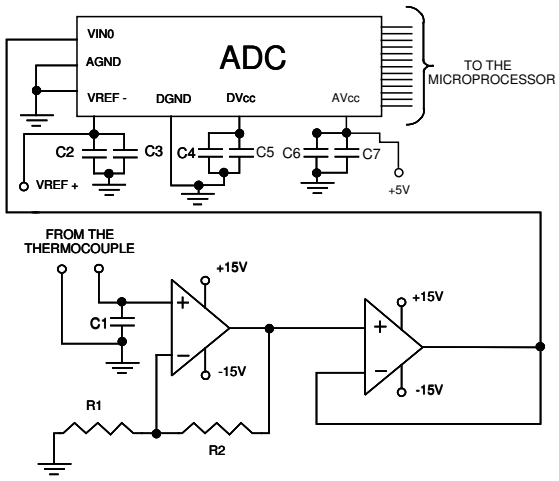

Fig. 9. Signal conditioning circuit

It is perhaps important to say that more detailed diagrams of this work can be found in Joers [2007]. Additionally, all of the data sheets describing the typical use of each one of these IC's can be obtained through the web site of the manufacturer, for example Atmel [2007] .

5. EXPERIMENTAL RESULTS

The experimental trace shown in Fig. 10 illustrates the dynamic characteristic of the furnace temperature following a 172 C reference command. We used here the same gains and closed-loop poles than those specified in Section 3. Initially, the furnace was at 33 C. The temperature begins to increase immediately until the temperature error is close to zero, which occurs approximately at 750 sec. Test shown in Fig. 10 was performed with a load inside the furnace chamber, therefore major parametric variations, other than those represented by Table I, were involved.

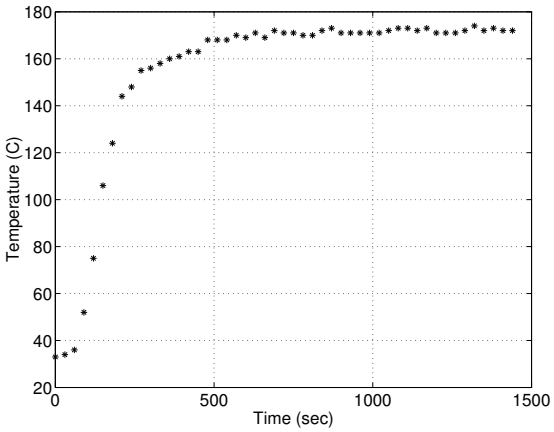

Fig. 10. Measured temperature during a test with load in the chamber. Closed loop poles: $z_{1,2} = 0.97, 0.965$.

Test was used to determine one physical property of an organic compound, Kirk et al [1991]. In particular, it was employed to obtain the melting point of the saccharose. For this purpose 156 gr. of that compound were placed into a 250 mL tube at the beginning of the test. Comparing Fig. 3 and Fig. 10 we conclude that the dynamics of the augmented system is slightly modified by the added mass of the tube-compound set. However, it is evident that the experimental overall system is still working well since the discrete integrator was able to compensate the parameter mismatch.

It is important to note that the closed loop settling time, shown in Fig. 10, has been reduced by the action of the state feedback. In open loop operation the settling time was about 4000 sec., see Fig. 2. In most of the cases, decreasing the settling time is a desired feature that reduces significantly the total time of the experiment. In industrial settings, that might be important since it diminishes the non-productive time of the chemical plant. In other cases, for example the anaerobic conversion of sugar to carbon dioxide and alcohol, this reduction of the settling time is just a small period of time compared to the total reaction time.

Additionally, there are compounds that have to be investigated by increasing the temperature in a controlled manner. In other words, a particular settling time is required. To accommodate these cases, different settling times having different sets of gains (corresponding to different sets of closed loop poles) were programmed in the microprocessor. Selecting a particular settling time is a feature that is available through the use of the keyboard and LCD.

Before doing any experiment all of the poles and gains were obtained and tested by using simulation as a tool. Figures 11 and 12 show two experimental transients associated with two settling times. The design specification for the settling time in Fig. 11 was 2500 seconds. This time is connected to the selection of the closed loop poles and gains: $z_{1,2} = 0.9925, 0.9020$ and $[K_I, K] = [0.0003, 0.0364]$, respectively. The initial temperature was 54 C and the set point was 215 C.

Figure 12 has a specified settling time equal to 3250

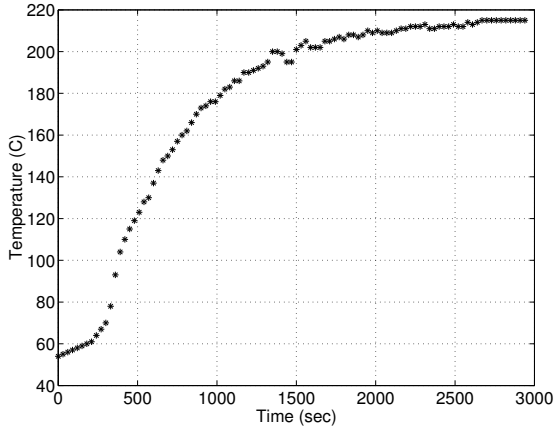

Fig. 11. Measured temperature during a test with no load in the chamber. Closed loop poles: $z_{1,2} = 0.9925, 0.9020$.

seconds and was obtained by using the following sets of poles and gains: $z_{1,2} = 0.9942, 0.9280$ and $[K_I, K] = [0.0001, 0.0267]$, respectively.

The initial temperature was 26 C and the set point was 330 C.

This particular hardware/software design does not considerer to make the integral error available for measurement, therefore no experimental transient is shown.

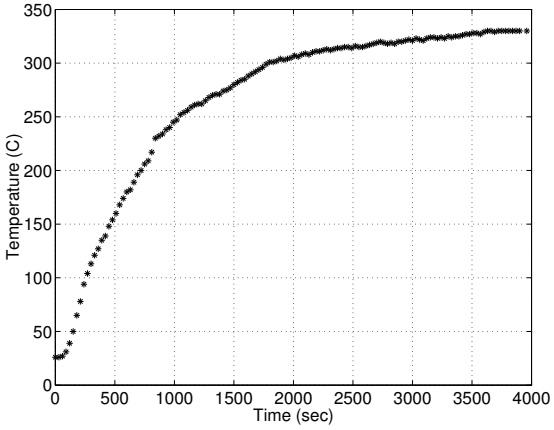

Fig. 12. Measured temperature during a test with no load in the chamber. Closed loop poles: $z_{1,2} = 0.9942, 0.9280$.

REFERENCES

N. Barry and E. McQuade, Temperature control using integer-cycle binary rate modulation of the AC mains. *IEEE Transactions on Industry Applications*, Vol. 31, No. 5, 1995.

E. Grassi and K. Tsakalis, PID controller tuning by frequency loop-shaping: application to diffusion furnace temperature control. *IEEE Transactions on Control Systems Technology*, Vol. 8, No. 5, 2000.

U.C. Moon and K. Y. Lee, Hybrid algorithm with fuzzy system and conventional Pi control for the temperature control of TV glass furnace, *IEEE Transactions on Control Systems Technology*, Vol. 11, No. 4, 2003.

Z. Huaiquan and W. Xing, The application of the embedded operating system at control of furnace, *Chinese Control Conference*, pp. 1959-1962, 2006

X. Gao, X. Cai and X. Yu, Simulation research of genetic neural network based PID control for coke oven heating, *Sixth World Congress on Intelligent Control and Automation*, pp. 7706-7710, 2006

H. Rashid Muhammed, *Power electronics: circuits, devices and applications*, Prentice Hall, 2004.

Barnstead Thermolyne Corporation, *Tube Furnace. Operation Manual and Parts List*, Madison, WI, 1997.

K. Ogata, *Discrete-Time Control Systems*, Prentice Hall, Englewood Cliffs, NJ; 1995.

G. F. Franklin, J. D. Powell and M. Workman, *Digital Control of Dynamic Systems*, Addison Wesley, Menlo Park, CA; 1998.

Mathworks, Inc. Matlab 6.1, 2001.

Chi-Tsong Chen, *Linear System Theory and Design*, Oxford University Press, New York; 1999.

R.F. Coughlin and F.F. Driscoll, *Operational amplifiers and linear integrated circuits*, Prentice Hall, 2001.

R.L. Boylestad and L.Nashelsky, *Electronic devices and circuit theory*, Prentice Hall, 2006.

C. A. Joers-Delgado, *Temperature control of a tube furnace*, MSc. thesis, in spanish. Instituto Tecnologico de Cd. Madero. Cd. Madero, Mexico; 2007.

Atmel Corporation, *AT89S8252 Microcontroller Data Sheet*, www.atmel.com , San Jose; 2007

R.S. Kirk, R. Sawyer and H. Egan, *Person's Composition and Analysis of Foods*, Addison Wesley, Menlo Park, CA; 1991.